LOW-FREQUENCY RIPPLE-SHAPING CONTROLLER FOR OPERATION OF NON-INVERTING BUCK-BOOST CONVERTERS NEAR STEP-UP STEP-DOWN BOUNDARY

Yuqing Zhang, Ivan Radović, S. M. Ahsanuzzaman, Aleksandar Prodić
Laboratory for Power Management and Integrated SMPS,
ECE Department, University of Toronto, CANADA
{yuqing.zhang, ivan.radovic}@mail.utoronto.ca,
{ahsansm,prodic}@ece.utoronto.ca

Giacomo Calabrese, Giovanni Frattini, Maurizio Granato
Texas Instruments
Freising, GERMANY & Milan, ITALY
{maurizio.granato, giovanni.frattini, g-calabrese}
@ti.com

***Abstract*— This paper introduces a practical controller for low power noninverting dc-dc buck-boost converters that minimizes the step-up step-down mode transition problem, while also significantly improving power processing efficiency compared to existing state-of-the-art solutions. Near the step-down step-up boundary, the controller enters a low-frequency ripple shaping mode of operation that allows lower operation frequency than in conventional buck or boost modes without paying a penalty of increased ripple, i.e. RMS, current. As a result, both switching and conduction losses are reduced. Furthermore, since the ripple shaping mode can cover both buck and boost modes of operation, mode toggling problems are practically eliminated. The effectiveness of the controller is demonstrated with a 1.8 V to 5 V input, 3.3 V/10W output experimental prototype where stable operation, smooth mode transitions, and power processing efficiency improvements of up to 6% are demonstrated.**

Keywords—dc-dc converter, ripple-shaping, digital controller

I. INTRODUCTION

For battery-powered portable applications like smart phones, portable audio players, laptops, etc., long battery operating time is required. In order to effectively use available battery capacity, a non-inverting buck-boost (Fig.1) is frequently used as a front-end stage in power management systems providing a well-regulated output bus voltage. While the battery is fully charged the converter operates in the buck. When its voltage drops below that of the bus, the converter usually switches into the boost mode, to maintain the same output voltage independent of the battery state of charge (SoC). Even though the converter can operate in the buck-boost mode directly, this mode is not desirable, mostly due to a significant drop in power processing efficiency and requirements for larger inductor current compared to the two other modes of operation.

However, the transition between the two modes has proven to be a challenging task [1], [2], [3], potentially causing undesirable mode toggling, drops in power processing efficiency, and EMI problems. Among the main reasons are the nonlinear characteristics of the converter around the full duty ratio for the buck mode and the zero duty ratio for the boost mode [4]. The nonlinearities are caused by the finite rise and fall times of the switching node voltages ($v_{x1}(t)$ and $v_{x2}(t)$ of Fig.1) limiting the minimum value of the duty ratio in the boost mode and causing saturation-like voltage conversion characteristic in the buck mode. Consequently, when V_{in} approaches V_{out}, there is a discontinuity in the transfer characteristic, which causes a pulse-skipping phenomenon and oscillation in the output voltage [4].

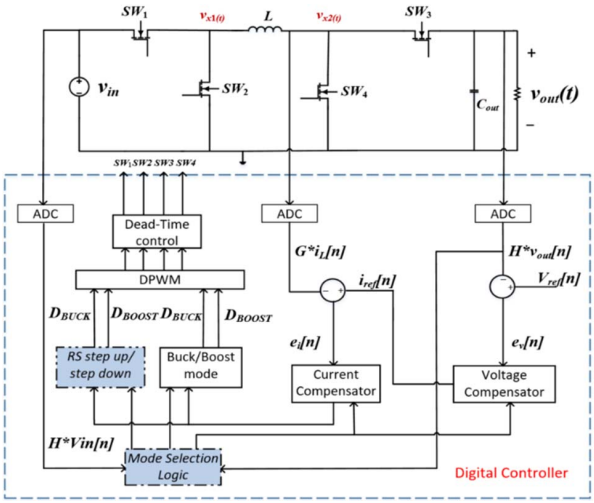

Fig. 1 Non-inverting buck-boost converter regulated with low-frequency ripple-shaping controller, implemented through digital average current mode controller.

To address this problem a number of control based solutions have been proposed [5]-[10]. In [5], a control scheme with adaptive switching frequency was proposed. However, variable switching frequency operation is usually undesirable in the targeted EMI sensitive applications.

The method presented in [6] introduces a three-state transition mode, which has three switching intervals with combined buck and boost modes that brings down the current level. The control scheme in [7] divided the transition mode into step-up and step-down and further reduces switching inductor current frequency to half while in the three-state transition mode. Both switching and conduction losses are reduced. However, four mode operation makes the mode transition challenging.

In [8], a mixed-mode transition has been proposed. When $V_{in} \approx V_{out}$, the controller switches between buck and boost

This work of Laboratory for Power Management and Integrated SMPS is supported by Texas Instruments.

modes sequentially. Although the pulse-skipping problem is minimized by mixed-mode operation, it still exists as the analog nature of this controller makes it difficult to set a limit on the duty cycle. At the edge of transition, the variation in the control voltage of the analog pulse width modulator, causes instability in the inductor current. State of the art commercial solutions also predominantly use mix mode controllers [9] and three-state transition mode [10].

The goal of this paper is to introduce a control method and its practical implementation, shown in Fig.1, that eliminates the previously mentioned mode transition stability problems and further improves power processing efficiency of buck-boost converters when $V_{in} \approx V_{out}$, as compared to existing state of the art solutions. In this case the digital averaged mode controller of Fig.1 has an additional third mode of operation. This mode is based on low-frequency ripple shaping that, even in the presence of heavy loads, maintains low current ripple while drastically reducing switching losses. It will be shown that this mode also reduces conduction losses, providing significant power processing efficiency improvements.

II. Principle of Operation

The introduced control scheme has three modes of operation and, depending on the mode, switches between two or three states shown in Fig. 2. When V_{in} is significantly larger than V_{out}, the converter operates in buck mode by switching between states 2 and 3, where SW_3 is on and SW_4 is off. When V_{in} is significantly smaller than V_{out}, it operates as a boost converter, by switching between state 1 and state 2, where SW_1 is always on and SW_2 is always off. When V_{in} is close to V_{out}, the converter operates in ripple-shaping mode, which switching sequence is demonstrated

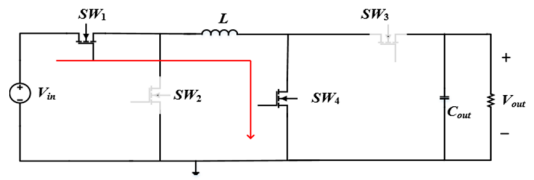

a. State1 inductor charging intervals

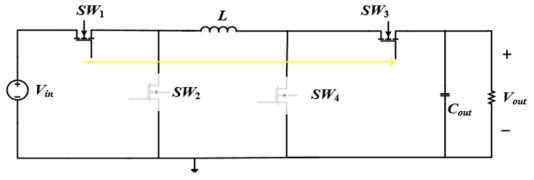

b. State 2 direct connection between input and output votlage

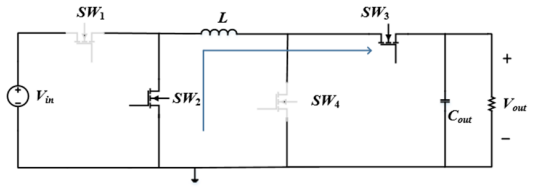

c. State 3 inductor discharging intervals

Fig. 2 Three states of a noninverting buck-boost converter power stage

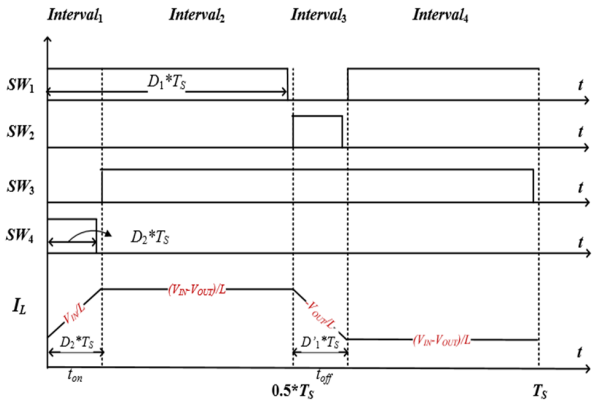

Fig. 3 Switching sequence and inductor current waveform in ripple-shaping mode.

by the diagrams of Fig.3. The regulation of the output voltage and mode switching is performed by the digital average current programmed mode (CPM) controller of Fig 1, as described in subsection II. B.

A. Gating sequence for steady state operation

The ripple-shaping concept has been proposed for the use in high power converters [11]. There, through alteration of the switching sequence, converter inductor current waveforms are modified, compared to their conventional shapes, to minimize the RMS current values, and therefore, reduce conduction losses. The current shaping switching sequence and corresponding waveforms used in this case, i.e. for the non-inverting buck boost of Fig. 1 when $V_{in} \approx V_{out}$, are shown in Figs. 2 and 3, respectively, where D_1Ts defines the transistor SW_1 on time and D_2Ts the on time of SW_4.

In this mode, the converter conversion ratio can be expressed with the following equation:

$$\frac{V_{out}}{V_{in}} = \frac{D_1}{1 - D_2} \quad , \qquad (1)$$

where D_1 is the ratio between the turn on time of SW_1 and period T_S, D_2 is the ratio between turn on time of SW_4 and period T_S. This equation shows that in the ripple shaping mode both step-up and step-down functions of the converter can be obtained. By looking at the waveforms of Fig. 3 another interesting feature can be noticed. It can be seen that, in addition to having ability to regulate the RMS current, for $V_{in} \approx V_{out}$ this mode also allows practically independent regulation of the current ripple and the switching frequency. This key feature of the ripple shaping (RS) mode is utilized to optimize the trade-offs between the switching and conduction losses and improve power processing efficiency compared to that of state of the art solutions [9], [10], while maintaining stable operation. According to the inductor volt-second balance [12], the relationship between the load current, I_{Load}, and the average inductor currents for the buck, boost, and ripple shaping modes are given by the following equations:

$$I_{L(ave)\_buck} = I_{LOAD} \quad , \qquad (2)$$

$$I_{L(ave)\_boost} = \frac{1}{D'_{boost}} I_{LOAD} \quad , \qquad (3)$$

$$I_{L(ave)\_rs} = \frac{1}{1 - \frac{t_{on}}{T_S}} I_{LOAD} \quad , \qquad (4)$$

where D_{boost} is the duty ratio of the converter when operating in boost mode, $t_{on} = D_1 Ts$ (Fig. 3) is the turn on time of SW_4, and T_S is the switching period. By looking at the equations it can be seen that for $T_S >> t_{on}$, the ripple-shaping mode has almost the same average current as a buck and lower average current than the boost, since in this case T_S consists of four intervals and for the same conversion ratio is longer than that of the boost. It should also be noted that, since the conversion ratio depends on both D_1 and D_2, by maintaining a constant small t_{on} or t_{off} time while reducing the switching frequency, the average inductor current can be further reduced in this mode.

B. Dual-frequency modulation

As discussed in the previous subsection, lower average inductor current can be obtained by lowering the switching frequency. Furthermore, it can be noticed that for $V_{in} \approx V_{out}$, by maintaining a constant t_{on}, the ripple amplitude can be kept at approximately the same level while reducing the switching frequency. Therefore, not only the switching losses but also the RMS current in the RS mode can be reduced, minimizing conduction losses. Hence, both switching losses and potentially conduction losses can be reduced, compared to the buck and boost cases. To utilize this advantage, in the introduced controller, dual-frequency operation is utilized. In RS mode, the converter operates at a lower switching frequency than that of the buck and boost. The lower frequency is selected based on the peak inductor current and ripple limitation and/or to be the same as an existing low-frequency mode of operation for a given converter that, in the targeted applications, is usually used for light load operating conditions. Examples include various schemes where the converter operates in the discontinuous conduction (DCM) at a much lower frequency than during heavy and medium load conditions.

III. Practical Implementation

The practical implementation of the ripple-shaping logic control is shown in Fig.1. The controller is a modification of a conventional average current programmed (CPM) controller containing an outer output voltage loop and an inner current regulation loop, both of which are digital. In this case, the controller also contains Mode Selection Logic that decides the mode of operation based on the converter operating conditions. Three ADCs are used for sensing the input voltage, the output voltage, and the inductor current. A digital equivalent of the attenuated output voltage $HV_{out}[n]$ is compared with the reference $V_{ref}[n]$. The voltage compensator then takes the resulting error $e_v[n]$ and sets the inductor current reference $I_{ref}[n]$. The current loop compensator compares $I_{ref}[n]$ to a digital equivalent of inductor current and, accordingly, provides the duty ratio control variable $d[n]$ to the digital pulse width modulator (DPWM) [12].

A. Mode selection logic

The *mode selection logic* (shown in Fig.1) is the key new element of the introduced controller. It chooses the most preferable operating mode according to the input voltage and output voltage with hysteretic band considered. Ripple-shaping control logic is bypassed when converter operates in buck or boost mode. When the converter operates in ripple-shaping step-up mode, the turn off time of SW_1 is fixed at a fixed small value, i.e. the minimum value. The turn on time of $SW_{3,4}$ is regulated by the compensator. While the converter is in ripple-shaping step-down mode, the turn on time of SW_3 is fixed at the minimum value and turn on time of $SW_{1,2}$ are calculated by the compensator. The buck switch pair $SW_{1,2}$ and boost switch pair $SW_{3,4}$ work sequentially with a 180 degree phase shift to shape the current into a trapezoid-like form, as shown in Fig. 3. The period of DPWM is extended, which decreases the effective switching frequency of the converter. Counter based DPWM is used to set the turn on or turn off time for $SW_{1\text{-}4}$.

A hysteretic band logic is used to avoid the mode toggling during transitions. The operation of the hysteretic band logic can be described with the help of the diagram of Fig. 4. When V_{in} is decreasing and becomes smaller than V_2, the mode of operation changes from buck to ripple-shaping mode and stays in the ripple-shaping until V_{in} is smaller than V_6. When V_{in} is increasing, the transition from boost mode to ripple-shaping happens when V_{in} is bigger than V_5 and stays at ripple-shaping until V_{in} is bigger than V_1. Similarly, within ripple-shaping mode, hysteretic band between step down and step up mode is also added. Hence, there is a large allowed range of variation between V_1 to V_2, V_3 to V_4, and V_5 to V_6 . It should be noted that this type of hysteretic transition is by its nature much less

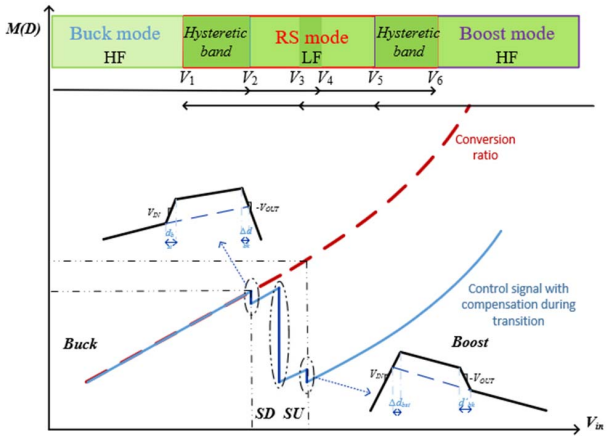

Fig. 4 Mode transition with hysteretic band and compensator reset, Vin is decreasing from V_1 to V_6

susceptible to mode toggling than those used in other solutions, since the converter does not change its voltage conversion function, so the problem is practically eliminated. In addition, transition between buck or boost to ripple-shaping includes frequency change and small duty ratio change. And compensator is reset for an almost seamless transition. For example, when the converter changes from buck or boost mode to ripple-shaping mode, the turn on time SW_1 or SW_4 is extended k times to accommodate the frequency change, where k is the frequency ratio between buck or boost mode to ripple shaping mode. Also, when mode changes from buck to RS step down, the duty ratio decreases due to the insertion of D_2T_S, i.e. turn on time of SW_4. Likewise, in transition from RS step down to buck, duty ratio increases. While in the transition from boost to ripple-shaping, duty-ratio is increased due to the operation of $SW_{1,2}$. Similarly, for the transition from RS step up to boost, the duty ratio is decreased as shown in the Fig.4. For ripple-shaping, compensator is reset to either minimum or maximum duty ratio value, in step up or step down during the transition.

III. Experimental Results

Table I: Converter parameters

Parameters	Value
V_{IN}	1.8[V]-5.5[V]
V_{OUT}	3.3[V]
I_{OUT}	0.5[A]-3[A]
$f_{Sbuck/boost}$	2[MHz]
f_{SRS}	200[kHz]
L	4.7[μH]
C_{OUT}	30[μF]

Based on the diagrams of Figs. 1 and 4, an experimental prototype has been built, to verify the operation of the introduced low-frequency ripple shaping based buck-boost controller. The controller was created using an FPGA-based evaluation board and the parameters of a custom-made discrete power stage are shown in Table I. Using the same power stage, the performance of the new controller is compared to the performances of the control methods used in two commercial state of the art solutions [9] [10]. Figs. 5 to 14 show the results of experimental measurements.

Figs. 5 to 8 show four distinctive modes of operation and transition, namely, ripple-shaping step down, ripple-shaping step up, boost, and buck, respectively. Figs. 9 to 13 show for mode transition between buck mode, boost mode and ripple-shaping mode. The results confirm fast and smooth mode transitions as well as stable operation in all modes. It can be seen that, even though the converter operates at 10 times lower switching frequency in ripple shaping mode compared to buck and boost (200 kHz vs. 2 MHz), the current ripples are still comparable. However, from the efficiency point of view large advantages are gained. Fig. 14 shows efficiency measurement comparison between the ripple shaping controller and the controllers used in two state-of-the-art commercial solutions [9] [10] for load currents varying from 0.5A to 3A and one-to-one voltage conversion ratio. Results show that that low frequency ripple-shaping control improves efficiency by about a 4% at lighter loads and by a 6% at heavy loads. The results for heavy load improvements indicate that both conduction and switching losses are reduced.

Fig. 5, V_{IN}=3.6V, V_{OUT}=3.3V, RS step-down mode. Ch1: Output voltage, V_{OUT} (5 V/div); Ch2: Inductor current, I_L (200m A/div); Ch3: Boost switching node (5V/div); Ch4: Buck switching node, V_{IN} (5 V/div)

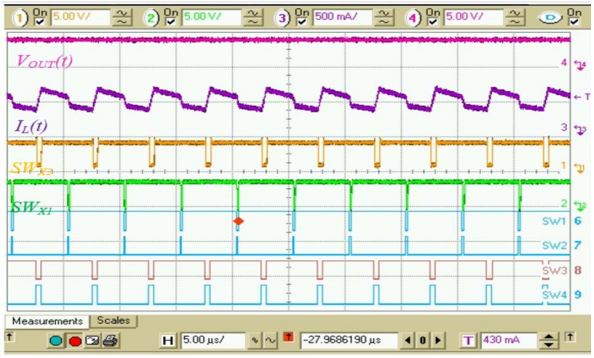

Fig. 6, V_{IN}=3V, V_{OUT}=3.3V, RS step-up mode. Ch1: Output voltage, V_{OUT} (5 V/div); Ch2: Inductor current, I_L (200m A/div); Ch3: Boost switching node (5V/div); Ch4: Buck switching node, V_{IN} (5 V/div)

Fig. 7, V_{IN}=2.2V, V_{OUT}=3.3V, Boost mode. Ch1: Output voltage, V_{OUT} (5 V/div); Ch2: Inductor current, I_L (200m A/div); Ch3: Boost switching node (5V/div); Ch4: Buck switching node, V_{IN} (5 V/div)

Fig. 8, V_{IN}=5V, V_{OUT}=3.3V, Buck mode. Ch1: Output voltage, V_{OUT} (5 V/div); Ch2: Inductor current, I_L (200m A/div); Ch3: Boost switching node (5V/div); Ch4: Buck switching node, V_{IN} (5 V/div)

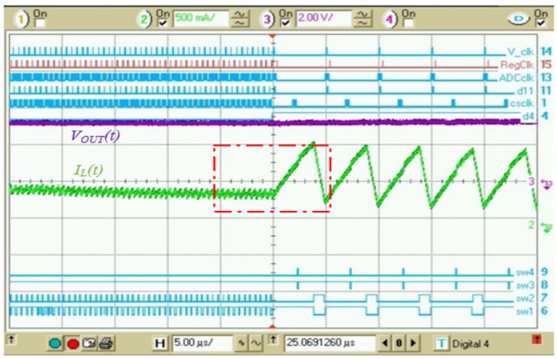

Fig. 9, V_{IN}=4V, V_{OUT}=3.3V, Mode transition from buck mode to RS step-down mode. Ch3: Output voltage, V_{OUT} (2 V/div); Ch2: Inductor current, I_L (500m A/div);

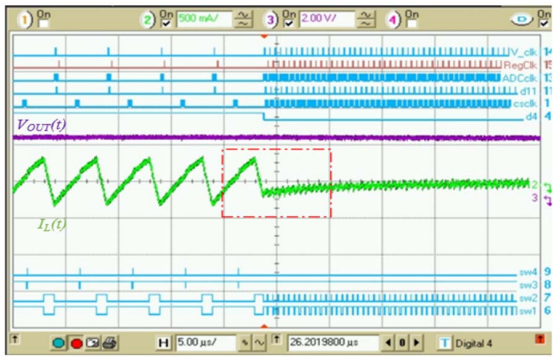

Fig. 10, V_{IN}=4.1V, V_{OUT}=3.3V, Mode transition from RS step-down mode to buck mode. Ch3: Output voltage, V_{OUT} (2 V/div); Ch2: Inductor current, I_L (500m A/div);

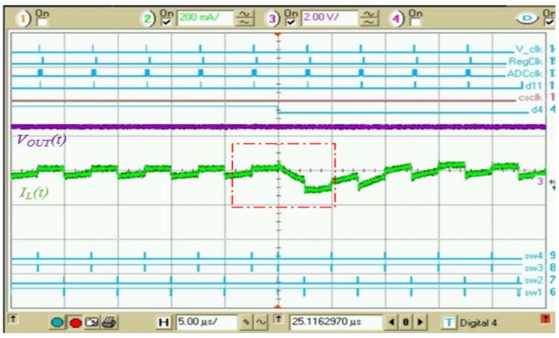

Fig. 11, V_{IN}=3.4V, V_{OUT}=3.3V, Mode transition between Step-down mode and Step-up mode. Ch3: Output voltage, V_{OUT} (5 V/div); Ch2: Inductor current, I_L (200m A/div);

Fig. 12, V_{IN}=2.9V, V_{OUT}=3.3V, Mode transition from RS step-up mode to boost mode. Ch3: Output voltage, V_{OUT} (2 V/div); Ch2: Inductor current, I_L (500m A/div);

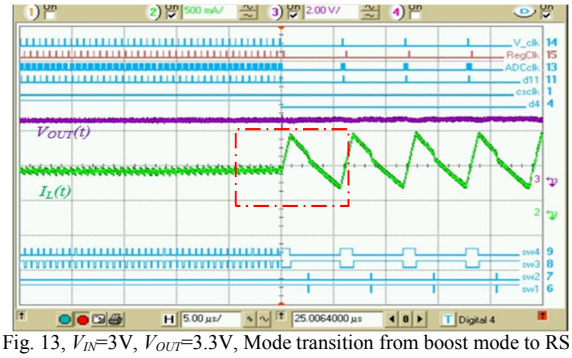

Fig. 13, V_{IN}=3V, V_{OUT}=3.3V, Mode transition from boost mode to RS step-up mode. Ch3: Output voltage, V_{OUT} (2 V/div); Ch2: Inductor current, I_L (500m A/div);

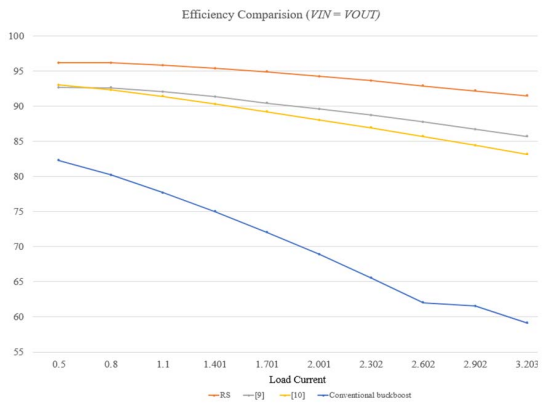

Fig. 14, Efficiency comparison between different control methods with load current from 0.5A to 3A

V. Conclusions

A low frequency ripple shaping control method for operation of non-inverting buck-boost converters near the boundary between the buck and boost modes is introduced. The method practically eliminates mode transition problems existing in commonly use solutions and, at the same time, improves power processing efficiency for conversion ratios close to one-to-one. These advantages are achieved by operating in a single mode that allows both step-up and step-down function and providing operation at low frequency with

low current ripple. Therefore, both conduction losses and switching losses are reduced.

REFERENCES

[1] X.-E. Hong, J.-F. Wu and C.-L. Wei, "98.1%-Efficiency Hysteretic-Current-Mode Noninverting Buck–Boost DC-DC Converter With Smooth Mode Transition," *IEEE Transactions on Power Electronics,* vol. 32, no. 3, pp. 2008-2017, 2017.

[2] Y.-J. Lee, A. Khaligh and A. Emadi, "A Compensation Technique for Smooth Transitions in a Noninverting Buck–Boost Converter," *IEEE Transactions on Power Electronics,* vol. 24, no. 4, pp. 1002 - 1015, 2009.

[3] K.-F. Wong and C.-H. Tsai, "A completely smooth transition Buck-Boost Converter with Continuity-Mode (CM) Technique for only using 2 switches in whole battery life," in *Power Electronics and Drive Systems (PEDS), 2011 IEEE Ninth International Conference on*, Singapore, 2011.

[4] R. Paul and D. Maksimovic, "Analysis of PWM Nonlinearity in Non-Inverting Buck-Boost Power Converters," in *PESC 2008*, Rhodes, Greece, 2008.

[5] D. C. Jones and R. W. Erickson, "Buck-Boost Converter Efficiency Maximization via a Nonlinear Digital Control Mapping for Adaptive Effective Switching Frequency," *IEEE Journal of Emerging and Selected Topics in Power Electronics,* vol. 1, no. 3, pp. 153 - 165, 2013.

[6] X. Hu and P. K. T. Mok, "Analysis and design of three-state controlled transition mode for a buck-boost converter with efficiency and stability enhancement," in *Circuits and Systems (ISCAS), 2013 IEEE International Symposium on*, Beijing, 2013.

[7] P.-C. Huang, W.-Q. Wu, H.-H. Ho and K.-H. Chen, "Hybrid Buck–Boost Feedforward and Reduced Average Inductor Current Techniques in Fast Line Transient and High-Efficiency Buck–Boost Converter," *IEEE Transaction on Power Electronics ,* vol. 25, no. 3, pp. 719-730, 2009.

[8] C.-L. Wei, C.-H. Chen, K.-C. Wu and I.-T. Ko, "Design of an Average-Current-Mode Noninverting Buck–Boost DC–DC Converter With Reduced Switching and Conduction Losses," *IEEE Transactions on Power Electronics,* vol. 27, no. 12, pp. 4934-4943, 2012.

[9] TEXAS INSTRUMENT, "TPS63070 2-V to 16-V Buck-Boost Converter With 3.6-A Switch Current," 2016. [Online]. Available: http://www.ti.com/general/docs/lit/getliterature.tsp?genericPartNumber=tps63070&fileType=pdf.

[10] MAXIM, "High-Efficiency, Seamless Transition,Step-Up/Down DC-DC Converter," 2009. [Online]. Available: https://datasheets.maximintegrated.com/en/ds/MAX8625-MAX8625A.pdf.

[11] J. W. K. Stefan Waffler, "A Novel Low-Loss Modulation Strategy for High-Power Bidirectional Buck ++ Boost Converters," *IEEE Transactions on Power Electronics ,* vol. 24, no. 6, pp. 1589 - 1599, 2009.

[12] R. W. Erickson, D. Maksimovic, Fundamentals of Power Electronics, New York: Springer-Verlag, 2001.

[13] A. Prodić, D. Maksimovic, R.W. Erickson "Design and implementation of a digital PWM controller for a high-frequency switching DC-to-DC power converter," in *Industrial Electronics Society, 2001. IECON '01. The 27th Annual Conference of the IEEE*, Denver, CO, USA, 2001.